Reverse Micellar Mass-Transfer Processes: Spray Column Extraction of Lysozyme

Gary J. Lye, Juan A. Asenjo, and D. Leo Pyle
Biotechnology and Biochemical Engineering Group, Dept. of Food Science & Technology, University of Reading, Reading, RG6 6AP, U.K.

Protein partitioning kinetics was measured for the semibatch extraction of lysozyme in a laboratory-scale, liquid–liquid spray column. The organic, isooctane phase contained reverse micelles formed from the anionic surfactant, sodium di-2-ethylhexyl sulfosuccinate. For the extraction of protein from aqueous to reverse micellar phases, experiments were performed over a range of dispersed-phase flow rates for cases of the organic- or aqueous-phase dispersion. The influence of aqueous-phase pH and ionic strength, which influence electrostatic interactions between protein and reverse micelles, was also investigated. Results were interpreted in terms of a two-film model of mass transfer. The nature of the dispersed phase could significantly influence the partitioning kinetics, while study of the droplet hydrodynamics suggested that stagnant drops were formed regardless of which phase was dispersed. Literature correlations for describing the droplet-formation process and droplet hydrodynamics predicted measured values satisfactorily. Attempts were also made to predict overall mass-transfer coefficients based on existing correlations describing mass transfer during droplet formation, free rise (or fall), and coalescence. Predicted values of K_L were 2–10 times greater than measured values, probably because of large concentrations of surfactant used to formulate the reverse micelle phases. This approach did, however, provide detailed information on the quantity of protein transferred during the successive processes of droplet formation, free rise (or fall) and coalescence.

Introduction

Reverse micelles are nanometer-sized aggregates of surfactant molecules in organic solvents. These surfactant aggregation structures are known to be thermodynamically stable and have been shown to be capable of solubilizing protein molecules without resulting in a loss of biological activity. Furthermore, both the extent and selectivity of this solubilization process have been shown to be influenced by a range of factors that include pH, ionic strength, and the nature of the surfactant used. The coexistence of aqueous and reverse micellar phases thus allows the application of liquid–liquid extraction technology to protein extraction and separation. The suitability of various liquid–liquid contacting devices such as mixer–settler units (Dekker et al., 1986) and membrane units (Dahuron and Cussler, 1988; Dekker et al., 1991a; Luthi and Hatton, 1991; Prazeres et al., 1993) for carrying out reverse micellar extractions has been shown on a laboratory scale. Only the use of centrifugal contacting devices (Dekker et al., 1991b) has been demonstrated on an industrial scale.

An alternative contacting device, which has been the focus of a very recent preliminary investigation, is a liquid–liquid spray column (Han et al., 1994). The advantages of these units are that they are simple to construct, have low capital costs, and are easy and flexible to operate (Lo, 1988). A particular advantage, when used with systems containing surfactants, is their low energy input; this circumvents problems of stable emulsion formation and the subsequent increase in phase disengagement times associated with mixer–settler systems. Problems of emulsion formation were recently encountered when the use of reverse micellar phases was investigated in a laboratory scale rotating disc contractor (Carneiro-da-Cunha

Correspondence concerning this article should be addressed to D. L. Pyle.
Current address of G. J. Lye: Department of Chemical Engineering, The University of Edinburgh, Kings Buildings, Mayfield Rd., Edinburgh EH9 3JL, U.K.

et al., 1994). Spray columns have also been recently investigated for protein extraction using aqueous two-phase systems (Rostami Jafarabad et al., 1992; Bhawsar et al., 1994), for the extraction of metal ions using emulsion liquid membranes (Uribe et al., 1988), and for the recovery of surfactant from waters used for *in-situ* soil flushing (Underwood et al., 1995). A disadvantage of spray columns, however, is that their design may produce axial mixing of the continuous phase that reduces extraction efficiency (Treybal, 1963). From a mass transfer point of view, spray columns also provide a system that is well characterized in terms of interfacial areas and droplet residence times. This allows calculation of mass transfer coefficients in a more practical situation than those measured in diffusion cells (e.g., Dekker et al., 1990; Dungan et al., 1991; Kinugasa et al., 1991) and permits investigation of the properties of the dispersed phase upon mass transfer. Both the dispersed-phase and continuous-phase mass-transfer coefficients will depend upon whether the dispersed-phase droplets are stagnant or circulating (Skelland and Caenepeel, 1972).

In this work, a mass-transfer model of protein extraction in a spray column has been developed to quantify the kinetics of protein extraction. This was based upon the two-film theory of mass transfer since it is known that this can be successfully applied to reverse micellar extraction (Dekker et al., 1986; Lye et al., 1994a). The column was operated in a semibatch mode (the continuous phase remained stagnant throughout each run) and the influence of aqueous-phase pH and ionic strength and the dispersed-phase flow rate upon lysozyme extraction kinetics was investigated. Under the conditions studied, the column operated at a very low dispersed-phase holdup; while this would be unrealistic in a processing situation, it does permit more accurate modeling of the column behavior. The physical properties of the various phases were also determined and the influence of the nature of the dispersed phase, either aqueous or organic, on droplet formation, droplet hydrodynamics, and protein mass-transfer rate was studied. The ability of existing literature correlations to describe droplet behavior and to predict overall mass-transfer coefficient was also investigated.

Materials and Methods

Precise details of materials and techniques used can be found elsewhere (Lye, 1993). Reverse micelle phases contained the surfactant sodium di-2-ethylhexyl sulfosuccinate, usually referred to as AOT (Sigma), in isooctane (Aldrich), while salts used in the aqueous phases were Anal-R grade (Merck). The lysozyme used was the Sigma Type II product (95% pure, pI 11.1, 14.4 kDa), which was assayed in both phases by absorption at 280 nm using experimentally determined extinction coefficients of $\xi_{aq} = 36{,}036$ and $\xi_{rm} = 36{,}894$ $cm^{-1} \cdot M^{-1}$. Water content of the reverse micelle phases was determined by Karl Fischer titration (Mettler, DL-37), results being presented as the molar ratio $W_0 (= H_2O]/[AOT])$.

Phases used in spray column experiments were preequilibrated in the absence of protein to ensure that the reverse micelle phase contained equilibrium concentrations of water and ions before the uptake of protein. Control experiments in which these phases were passed through the spray column showed that the W_0 value of the reverse micelle phase did not change significantly with time. Neither in these experiments, nor ones in which protein extraction occurred, was any interfacial precipitate observed. Equilibrium values of the lysozyme partition coefficient between the two phases were determined for extractions carried out in well-mixed systems at $V_r = 1$ ($V_r = V_{rm}/V_{aq}$), total phase volume ≈ 100 mL, in which phase separation occurred in an incubator at 25°C. Equilibrium lysozyme concentrations were subsequently determined in both phases by UV absorption. Physical properties of these phases were measured at 25°C before and after phase equilibration. Phase densities were determined using a 25-mL density bottle (maximum standard deviation = 0.0002), while viscosities were measured using a u-tube viscometer (Technico BS/U-A) (maximum standard deviation = 0.005). Interfacial tensions were measured using a Kruss K12C tensiometer fitted with an RI-12 interfacial tension ring (maximum standard deviation = 0.02). Measurements made over a period of 30 minutes, after creating the interface, showed no significant variation.

Description of equipment

The spray column and ancillary vessels (as shown in Figure 1) were of all-glass construction and were connected by Viton tubing. A second identical column was also used that had sample points every 10 cm, up to a height of 60 cm, to facilitate sampling of the continuous phase as a function of height. All equipment was thoroughly rinsed in deionized water and dried before use. The dispersed-phase flow rate was controlled using a stainless-steel gap meter fitted with Viton seals (Platon, Model GTV) which was calibrated using the appropriate dispersed phase (Lye, 1993). Droplet counts from each nozzle, taken at timed periods throughout a run, showed that the distribution of dispersed phase through each nozzle was accurate to $\pm 6\%$.

Operational procedures

It was ensured that the column was mounted vertically and, as far as possible, that the droplets passed through the column without coalescing or contacting the column walls. The column was operated in semibatch mode with the continuous phase staying stagnant throughout each run, the dispersed phase flow rate being checked by measuring the volume of dispersed phase collected over time (the variation in the measured/set flow rates was smaller than $\pm 10\%$). During a typical experiment, in which the organic phase was dispersed, the dispersed phase would be sampled at various time intervals over 30 min, the samples being analyzed for protein concentration and water content. The continuous aqueous phase, which was generally only sampled before and after each experiment, was analyzed for protein concentration and pH (no pH change was recorded over the duration of the experiments). The change in average continuous-phase protein concentration, C_{aq}, with time, was calculated from the following mass balance:

$$V_{aq}C_{aq}(t) = V_{aq}C_{aq}(0) - Q_{rm}\int_{t(0)}^{t(t)} C_{rm}\,dt, \qquad (1)$$

where Q_{rm} is the flow rate of the dispersed phase and C_{rm} is the protein concentration in the reverse micelle phase (based

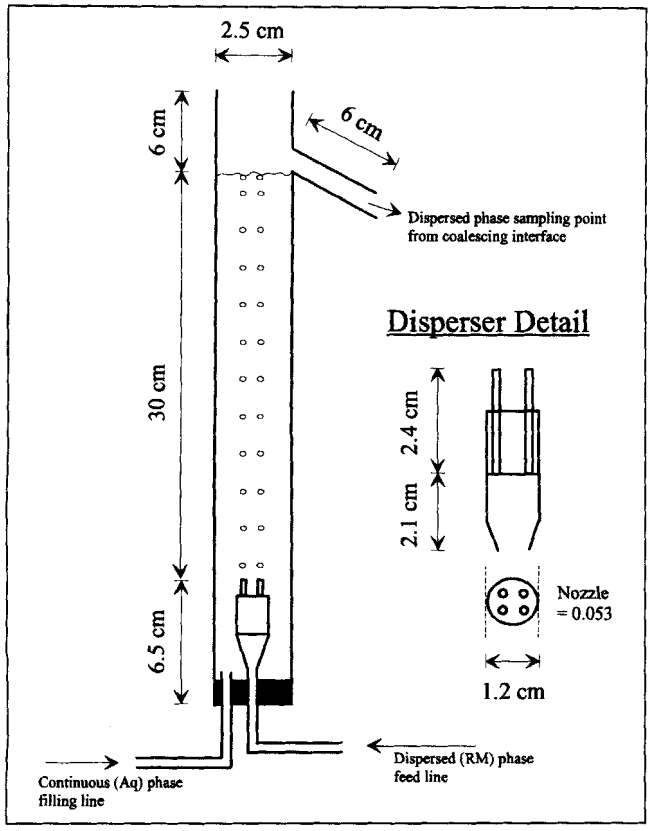

Figure 1a. Dimensions of the spray column and disperser for dispersed reverse micelle phases.

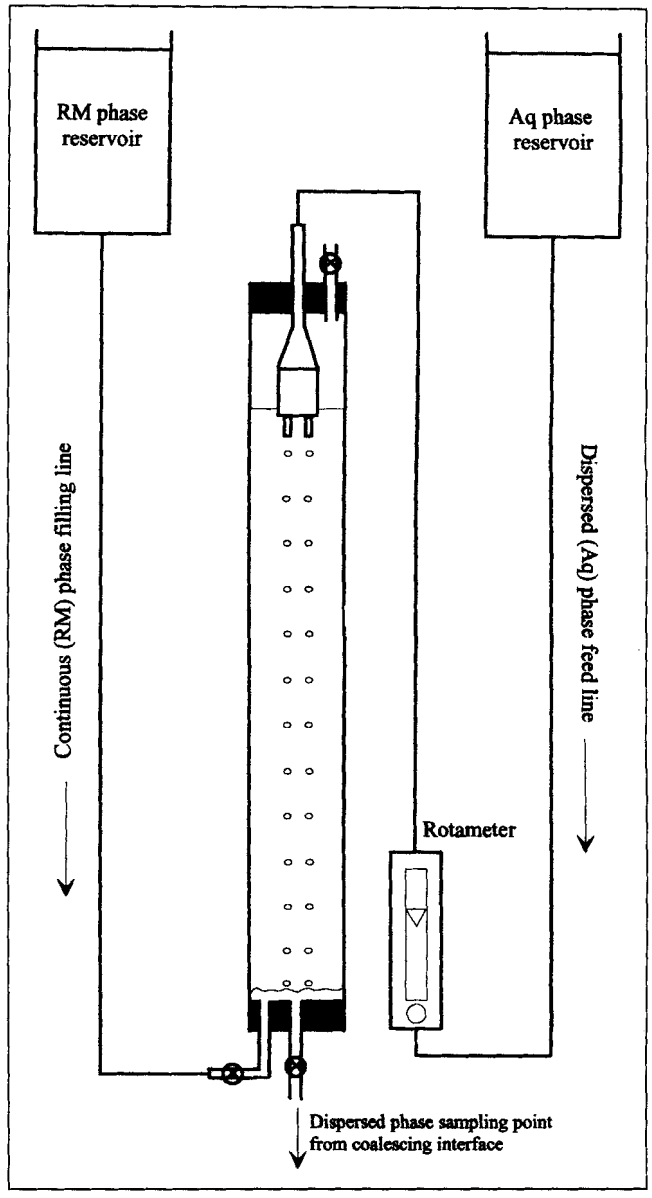

Figure 1b. Ancillary vessels for dispersed aqueous phases.

on its overall volume) at the top of the column. It is assumed that V_{aq} is constant and that the dispersed-phase holdup is negligible. Experimental protein mass balances at the end of each experiment were generally accurate to $100 \pm 10\%$. The residence time of the droplets in the column was also measured in each experiment so that a mean rising (or falling) velocity could be calculated. It is assumed that measurements made over the height of the 30-cm column allow calculation of a representative droplet terminal velocity, U_t.

Measurement of droplet sizes

The sizes of the dispersed-phase droplets were recorded photographically using a Minolta X300-S SLR camera fitted with a Tokina S2 70-210 macrolens and extension tubes. The column was fitted with a water-filled, rectangular, viewing chamber so that the images of the droplets were not distorted by the column walls and a measuring scale was located in the same plane as the center of the disperser. Once the film was developed, sizes of the individual droplets were measured using an image-analysis system consisting of the following: a Hitachi CCTV video camera, Mitsubishi video copy processor (Model P100B), and a PC running Oxford Framestore Applications software (OFA-III, version 2.20). The measuring function of the software was calibrated using the scale included in each photograph. For each droplet appearing on a photograph, except those that were close to the disperser, both horizontal and vertical diameters were measured. The surface area and volume of each droplet was then calculated, assuming them to be oblate spheroids (Weast, 1964). For each experiment, the sizes of 20–30 droplets were measured so that the calculated means of droplet surface area or volume no longer changed significantly by the inclusion of another set of measurements (t-test analysis showed that the means were not significantly different at the 5% level). For mean droplet surface areas, normalized standard deviations were between 6–14%, while for mean droplet volumes, normalized standard deviations were between 10 and 20%.

Since the dispersed-phase holdup was very small, $\approx 1\%$ v/v, it was not possible to accurately determine this by measuring the change in height of the continuous phase with and without the dispersed phase being passed through the column. Instead, both the specific holdup and specific interfacial area were determined from photographs of the droplets. For each experiment, values of the mean droplet surface area and vol-

ume, together with the number of droplets present in a given volume of the continuous phase, were used to calculate the specific interfacial area and specific holdup, respectively. Control experiments in which droplet sizes were measured throughout a run, showed very little variation in the calculated values of specific interfacial area (±5%) or specific holdup (±6%). Other control experiments showed similar variation in droplet sizes measured at the top and at the base of the 30-cm column.

Theory

The model described below is developed for a case in which the reverse micelle phase is dispersed in a continuous aqueous phase.

Mass-transfer rate to a single drop

Consider the partitioning of a protein to an organic phase droplet rising through a continuous aqueous phase. Assuming that the two-film theory of mass transfer applies, then the concentration of protein at the interface between the two phases, $C(i)$, will be at equilibrium and a partition coefficient, m, can be defined as

$$m = \frac{C_{aq}(i)}{C_{rm}(i)}. \tag{2}$$

The corresponding bulk concentrations of protein are given by C_{aq}, and C_{rm}, respectively, and smaller values of m represent a higher partition of protein to the reverse micelle phase. The overall mass-transfer rate per unit surface area is thus described by

$$j = K_L\left(\frac{C_{aq}}{m} - C_{rm}\right) = K_L(C^*_{rm} - C_{rm}), \tag{3}$$

where j is the protein flux, C^*_{rm} is the equilibrium protein concentration in the dispersed, reverse micelle phase, and K_L is the overall mass-transfer coefficient defined as

$$\frac{1}{K_L} = \frac{1}{k_{rm}} + \frac{1}{mk_{aq}}. \tag{4}$$

Under the experimental conditions employed, the value of m will be very small, and hence the forward transfer of protein is limited by diffusion in the aqueous boundary-layer film (Dekker et al., 1990; Kinugasa et al., 1991; Plucinski and Nitsch, 1989; Lye et al., 1994a). No term for the interfacial solubilization of protein is therefore included in Eq. 4. However, if the column were to be operated at higher values of pH or ionic strength than will be used here, then the interfacial kinetics may be sufficiently slow that a term representing the interfacial solubilization process would be necessary in Eq. 4.

Mass balance on a single drop

Consider an organic-phase droplet with surface area S, and volume V, which has steadily risen a distance, z, through a stagnant continuous phase that has a protein concentration C_{aq}. Assuming that S, V, and C_{aq} are constant with height during any droplet rise time, then if the mass transfer rate is given by Eq. 3 and U_t is the terminal drop velocity, a mass balance on the drop yields

$$V\frac{dC_{rm}}{dt} = VU_t\frac{dC_{rm}}{dz} = K_L S(C^*_{rm} - C_{rm}). \tag{5}$$

Integrating Eq. 5 between the limits $C_{rm}(0)$ and $C_{rm}(z)$ gives

$$C_{rm} = C^*_{rm}[1 - \exp^{-\alpha z}], \tag{6}$$

where

$$\alpha = \frac{K_L S}{VU_t}. \tag{7}$$

Equation 6 thus relates the protein concentration within the droplet, C_{rm}, to the height, z, that the droplet has risen up the column. Given the earlier assumption that C_{aq} was constant, it follows that C^*_{rm} will also be constant with height for any droplet rise time. The equilibrium protein concentration within the droplet C^*_{rm}, is estimated from the equilibrium partition coefficient, m, defined as in Eq. 2. For experiments in which the variation of droplet protein concentration is known with height, the overall mass-transfer coefficient can be estimated by rearranging Eq. 6 to

$$Ln\left(1 - \frac{C_{rm}}{C^*_{rm}}\right) = -\alpha z. \tag{8}$$

Thus, if the two-film theory is applicable in this case, a plot of $Ln(1 - C_{rm}/C^*_{rm})$ against z should yield a straight line and α (and hence K_L) can be estimated by linear regression.

Mass balance on the spray column

Consider a spray column of volume V_c, containing an aqueous phase that has a protein concentration $C_{aq}(t)$ at time t. The dispersed, reverse micelle phase enters the column with a volumetric flow rate, Q, such that each droplet formed at the disperser rises once through the column, emerging with a protein concentration C_{rm}. Under the experimental conditions employed, protein transfer is from the continuous phase to the dispersed phase, and initially, $C_{aq}(0)$ was 0.5 mg/mL and C_{rm} was zero. Assuming that the liquid in the continuous phase is perfectly mixed, a mass balance on the protein in the column gives

$$V_c = \frac{dC_{aq}}{dt} = -QC_{rm}. \tag{9}$$

Substituting for C_{rm} from Eq. 6 to account for the change in droplet protein concentration with height, and integrating between the limits $C_{aq}(0)$ and $C_{aq}(t)$ yields

$$\frac{C_{aq}(t)}{C_{aq}(0)} = \exp^{-\beta[1 - \exp^{-\alpha z}]t}, \tag{10}$$

Table 1. Physical Characterization of the Phases Used in Spray Column Experiments Before and After Protein Extraction*

RM Phase Equil. with	Before Extraction			After Extraction		
	Dens. (g/cm^3)	Vis. (mPa·s)	W_0 $[H_2O]/[AOT]$	Dens. (g/cm^3)	Vis. (mPa·s)	W_0 $[H_2O]/[AOT]$
0.2 M pH 7	0.7100	0.577	11.9	0.7106	0.578	10.8
0.3 M pH 7	0.7097	0.576	10.6	0.7102	0.577	10.0
0.4 M pH 7	0.7101	0.574	9.9	0.7103	0.575	9.6
0.2 M pH 9.4	0.7109	0.580	12.5	0.7108	0.579	11.7
0.2 M pH 10.6	0.7111	0.581	12.9	0.7109	0.580	12.0
None†	0.7076	0.565	0.4	0.7109	0.577	11.6
Aqueous Phase (+0.5 mg/mL Lysozyme)	Before Extraction			After Extraction		
	Dens. (g/cm^3)	Vis. (mPa·s)		Dens. (g/cm^3)	Vis. (mPa·s)	
0.2 M pH 7	1.0222	1.022		1.0220	1.020	
0.3 M pH 7	1.0277	1.055		1.0276	1.022	
0.4 M pH 7	1.0332	1.058		1.0331	1.026	
0.2 M pH 9.4	1.0210	1.021		1.0209	1.021	
0.2 M pH 10.6	1.0216	1.030		1.0215	1.023	
0.2 M pH 7 (NP)‡	1.0221	1.020		—	—	

*(Top) Reverse micelle phases of 50 mM AOT in isooctane and (bottom) aqueous phases of 90% KCl, 10% buffer (potassium phosphate, pH 7, or sodium carbonate/bicarbonate, pH 9.4 and pH 10.6). See Methods section for experimental details.
†Subsequently extracted with an aqueous phase of 0.2 M, pH 7.
‡NP: Contains no protein.

where

$$\beta = \frac{Q}{mV_c}. \tag{11}$$

Equation 10 therefore provides a relationship between the initial protein concentration in the column, $C_{aq}(0)$, and the concentration of protein remaining at time t, $C_{aq}(t)$, for a column of height z. Values of the only unknown, α (and hence K_L), were estimated by fitting Eq. 10 to $C_{aq}(t)$ data using an iterative, nonlinear curve-fitting procedure (Marquardt–Levenberg algorithm) in the software package Sigma Plot (Jandel Scientific).

Results and Discussion

Physical characterization of the phases and equilibrium protein partitioning

The physical properties of the aqueous and organic phases used in spray-column experiments are shown in Table 1 (results for the reverse micelle phase before extraction represent phases that have been preequilibrated as described earlier, and these measurements will be characteristic of the phases as they enter the spray column). The importance of measuring such properties in this kind of study, is that it will permit the subsequent use of general correlations for predicting the sizes of the droplets created, their terminal velocities, and the mass-transfer rates to and from such droplets. As will be shown in the following sections, this is particularly important in this work where correlations developed for conventional, aqueous–organic, two-phase systems will be evaluated for their applicability to the newly developed aqueous–reverse micelle systems used here.

The phase densities and viscosities, measured before and after protein extraction, show very little variation for both aqueous and organic phases and are consistent with the quantity of water, protein, and ions present in each sample. The unexpected result is the decline in water content of the reverse micelle phases after extraction, since they were preequilibrated with aqueous phases at the desired pH and ionic strength. This is probably due to the displacement of water molecules by solubilized protein rather than loss of surfactant molecules from the organic phase (no interfacial precipitate was observed and the aqueous phases showed no cloudiness). Results on the interfacial tension between the various phases, displayed in Table 2, again only show slight variations when determined before and after protein extraction. There is, however, a clear trend for the interfacial tension to increase with increasing aqueous phase ionic strength, due to an increase in film rigidity (Binks et al., 1989), and to decrease with increasing pH. Since these measurements were independent of time, the results are consistent with an interface saturated with a monolayer of surfactant molecules (Aveyard et al., 1986). Interfacial tensions measured in the absence of AOT were of the order of 35 $mN \cdot m^{-1}$.

Table 2 also describes the equilibrium partitioning of lysozyme between the two phases at $V_r = 1$ (in well-mixed sys-

Table 2. Interfacial Tensions and Equilibrium Protein Partitioning between Various Aqueous and Reverse Micelle Phases*

Two-Phase System	Interfacial Tension ($mN \cdot m^{-1}$)		Lysozyme Partitioning	
	Before Extraction	After Extraction	Mass Bal. (%)	m (C_{aq}/C_{rm})
0.2 M pH 7	1.49	1.48	101	0.026
0.3 M pH 7	1.60	1.63	98	0.025
0.4 M pH 7	1.75	1.78	104	0.053
0.2 M pH 9.4	1.27	1.22	98	0.032
0.2 M pH 10.6	1.16	1.03	98	0.056
0.2 M pH 7 (N)†	1.42	1.41	99	0.033

*See Table 1 and Methods section for experimental details.
†N: RM phase not preequilibrated.

tems) and indicates a strong dependence on electrostatic interactions between protein and surfactant molecules. Protein uptake by the reverse micelle phase is greater at low pH where there is a large negative charge on the protein surface, and at low ionic strength where there is little screening of the charges by added electrolyte (Dungan et al., 1991). Note that for all the systems used here, the conditions favor virtually complete uptake of the protein by the reverse micelles if the phases were allowed to reach equilibrium, although the kinetics of the processes would be different (Lye et al., 1994a).

Description of droplet formation

In liquid–liquid extraction processes such as the one occurring in the spray column used here, prediction of the droplet size, and hence the interfacial area, is important in order to evaluate solute mass-transfer coefficients. Having experimentally determined the physical properties of the phases (Tables 1 and 2) and measured the sizes of the droplets formed in the column (for raw data, see Lye, 1993), it is possible to examine existing correlations for predicting drop size and decide upon their suitability for modeling reverse micellar systems. In the case of droplet formation from a nozzle at low linear velocities where discrete, uniformly sized droplets are formed and no jetting occurs, Hayworth and Treybal (1950) proposed the following correlation:

$$V_d + 4.11\times10^{-4}V_d^{2/3}\left(\frac{\rho_d v^2}{\Delta\rho}\right) = 21\times10^{-4}\left(\frac{\sigma d_n}{\Delta\rho}\right) + 1.069\times10^{-2}\left(\frac{d_n^{0.747}v^{0.365}\mu_c^{0.186}}{\Delta\rho}\right)^{3/2}, \quad (12)$$

where the volume of the detached drop, V_d, is related to the linear velocity of the dispersed phase through a nozzle, v, the internal diameter of the nozzle, d_n, and the physical properties of the phases. In their experiments, these authors used low concentrations of an oil-soluble surface active agent (Alkaterge C) in order to study the effect of interfacial tension, σ, on the droplet-formation process. In a more recent study, Scheele and Meister (1968) used 15 liquid–liquid systems in order to investigate a wider range of variables than in previous works. They developed the following correlation that is particularly recommended for use in low-viscosity systems (Skelland, 1992):

$$V_d = F\left[\frac{\pi\sigma d_n}{g\Delta\rho} + \frac{20\mu_c Q d_n}{d_c^2 g\Delta\rho} - \frac{4\rho_d Q v}{3g\Delta\rho} + 4.5\left(\frac{Q^2 d_n^2 \rho_d \sigma}{(g\Delta\rho)^2}\right)^{1/3}\right], \quad (13)$$

where Q is the volumetric flow rate of the dispersed phase, F is the Harkins–Brown correction factor, which is taken as 0.625 in most cases (Skelland, 1992), and the drag term (containing the continuous phase viscosity, μ_c) can be neglected in this case since $\mu_c < 10$ cp.

An example of the effect of dispersed-phase linear velocity on the measured droplet sizes is shown in Figure 2 together with the predictions obtained from Eqs. 12 and 13. Both correlations predict the observed increase in V_d with increasing

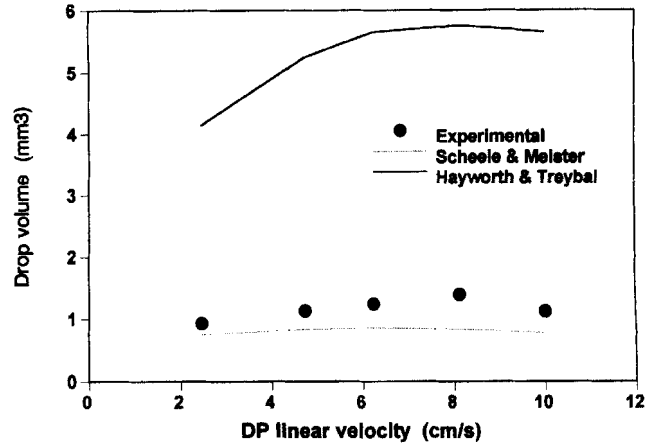

Figure 2. Effect of dispersed-phase (reverse micelle) linear velocity on measured drop volumes.

Predictions from Eqs. 12 and 13 were calculated using physical data for the phases before extraction. Aqueous phase initially consisted of 0.48 mg/mL lysozyme in 0.2 M 90% KCl/10% potassium phosphate buffer, pH 7, while the organic phase consisted of 50 mM AOT in isooctane.

linear velocity up to 8 cm s^{-1}, but the magnitude of the drop sizes predicted from Eq. 13 are far closer to the experimental values than those predicted by Eq. 12. A parity plot of predicted and measured droplet sizes for both equations over the complete range of conditions used in this study is shown in Figure 3. The Scheele and Meister correlation would appear to offer the closest predictions to the measured drop volumes, but there is a consistent underprediction of V_d (average error of 43%) and relatively little sensitivity to the range of operating conditions employed. Equation 13 is, however, known to underpredict values of V_d for small-diameter nozzles and low flow rates as used in this work.

Description of droplet hydrodynamics

The physical properties of the various phases described earlier can be correlated with the measured droplet sizes (see

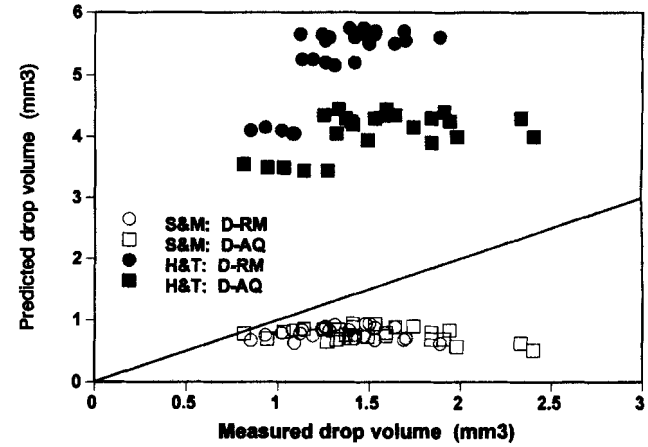

Figure 3. Parity plot of measured and predicted drop volumes.

Predictions from Eqs. 12 (Hayworth and Treybal) and 13 (Scheele and Meister) were calculated using physical data for the phases before extraction.

Figure 3) and their terminal velocities, U_t. Measured values of U_t were in the range of 0.07–0.11 ms^{-1} and were larger in the case of dispersed aqueous phases (for raw data see Lye, 1993). Droplets containing surface-active agents have reduced terminal velocities compared to those in "pure" systems (Skelland et al., 1987; Weatherley and Turmel, 1992)—the accumulation of surfactant molecules at the interface will tend to reduce internal circulation of the droplet by increasing the rigidity of the interface. This effect will be greatest in low viscosity phases, as used here, where the AOT forms a saturated monolayer at the interface, regardless of which phase is dispersed, and will be important later with regard to the selection of appropriate mass-transfer coefficients.

A wide range of correlations have appeared in the literature (Clift et al., 1978) describing droplet hydrodynamics. Grace et al. (1976) developed the following correlation for ellipsoidal fluid particles in systems that had been "contaminated" with surface-active agents. This was based upon earlier work in which relatively impure phase components had been used (e.g., Klee and Treybal, 1956; Hu and Kintner, 1955). The correlation applies for conditions where $M < 10^{-3}$, $Eo < 40$, and $Re > 0.1$, and is given in two parts:

$$J = 0.94H^{0.757} \quad \text{for} \quad 2 < H < 59.3 \tag{14}$$

and

$$J = 3.42H^{0.441} \quad \text{for} \quad H > 59.3, \tag{15}$$

where

$$H = \frac{4}{3} EoM^{-0.149} \left(\frac{\mu}{\mu_w} \right)^{-0.14} \tag{16}$$

and

$$J = ReM^{0.149} + 0.857, \tag{17}$$

where Eo is the Eötvös number, $g\Delta\rho d_e^2/\sigma$; M is the Morton number, $(g\mu^4\Delta\rho)/(\rho^2\sigma^3)$; Re is the Reynolds number, $(\rho d_e U_t)\mu$; and μ_w is the viscosity of pure water (Eo, M, and Re are defined in the nomenclature, while μ_w is taken as 0.0009 $kg \cdot m^{-1} \cdot s^{-1}$). Correlations on the behavior of rigid oblate spheroids have generally been developed for regularly shaped particles having a constant aspect ratio, E. In the experiments described here, E changes with phase composition and dispersed-phase flow rate. For conditions where the drag coefficient is virtually constant ($10^3 < Re < 10^4$), the following correlation was proposed (Clift et al., 1978):

$$U_t = 1.73 \left[\frac{\Delta\rho g E d}{\rho[1 + 1.63(1-E)^2]} \right]^{1/2} \tag{18}$$

Equation 18 is used here, as it permits calculation of U_t at various values of E even though experimental values of the Reynolds number were in the range $10^2 < Re < 10^3$.

Terminal velocity data plotted according to the correlation of Grace et al. (1976), that is, Eqs. 14–17, is shown in Figure 4. No significant difference was found when values of the

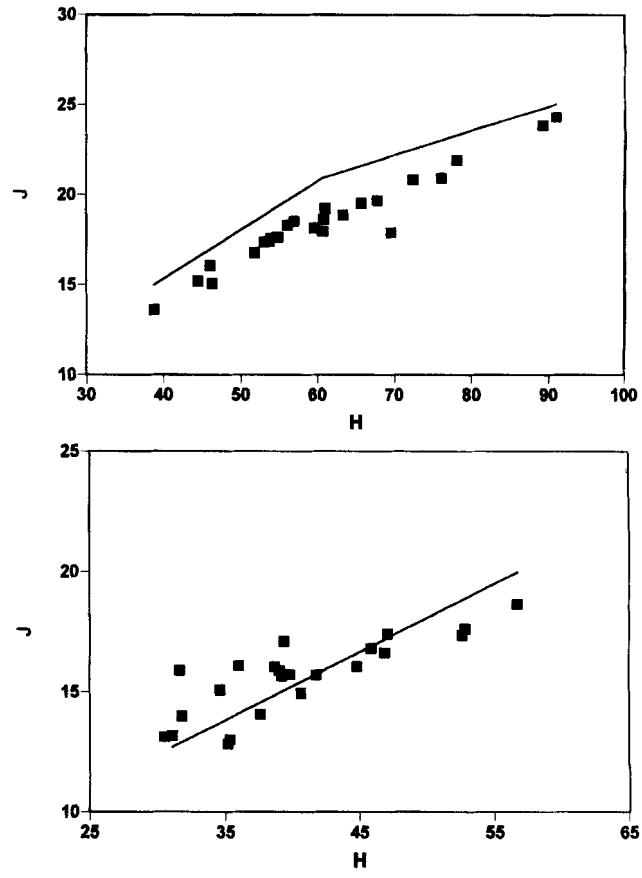

Figure 4. Droplet terminal velocity data for (top) dispersed aqueous phases and (bottom) dispersed reverse micelle phases.

Solid lines calculated from Eqs. 14 and 15 using experimental extraction data for phases before extraction.

physical properties of the phases were taken before or after protein extraction (Tables 1 and 2). The agreement between experimental data and the correlation is rather good considering the limitations in the determination of U_t stated earlier. Values of U_t calculated from the correlation of Clift et al. (1978), that is, Eq. 18, showed similar results, with predicted values of U_t generally being 10–15% greater than experimental values. The tendency for experimental values of U_t to be less than those predicted by the correlations is probably due to droplet–droplet interactions; both correlations were developed from data related to single-droplet studies. This agreement between experimental and calculated values of U_t, for both of the preceding correlations, suggests that the presence of surfactant in the system reduces internal circulation within the droplets for both dispersed-aqueous and organic phases.

Testing the model

In order to justify the assumptions built into the mass-transfer model and verify the application of the two-film theory, it is necessary to compare experimental extraction data with that calculated from the model. As described by Eqs. 6 and 10, α and hence K_L can be estimated in two ways: from data relating the change in droplet protein concentration with height or from data relating the change in continuous-phase

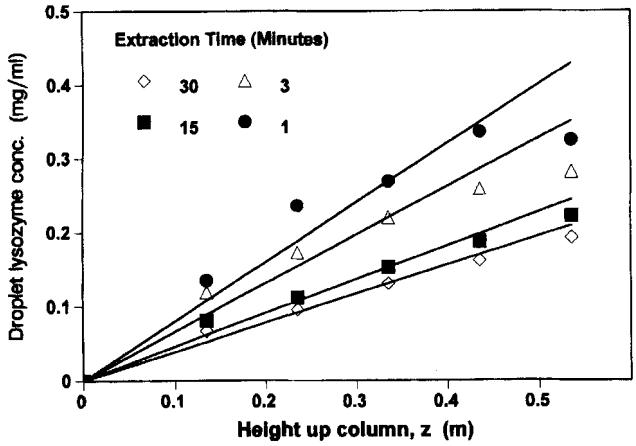

Figure 5. Variation of droplet protein concentration with distance risen through column.

Solid lines calculated from Eq. 6. Aqueous phase initially consisted of 0.48 mg/mL lysozyme in 0.2 M 90% KCl/10 % potassium phosphate buffer, pH 7, while the organic phase consisted of 50 mM AOT in isooctane. Dispersed phase flow rate was 4.3 mL/min.

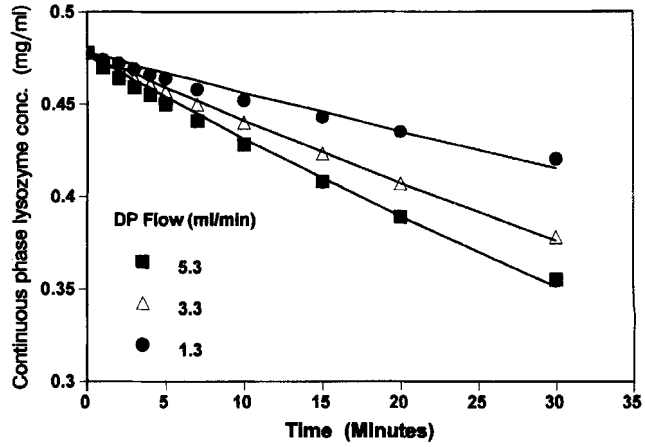

Figure 6. Effect of dispersed-phase flow rate on protein extraction from the continuous phase with time.

Solid lines calculated according to Eq. 10. Aqueous phase initially consisted of 0.48 mg/mL lysozyme in 0.2 M 90% KCl/10% potassium phosphate buffer, pH 7, while the organic phase consisted of 50 mM AOT in isooctane. Column height was 30 cm.

protein concentration with time. Since experiments were performed under identical conditions, calculated values of K_L should be the same in both cases.

Typical results for the change of droplet protein concentration with height and extraction time are shown in Figure 5 (for clarity, data are only shown at four extraction times). These data were obtained using columns of different heights, hence each experimental point includes the effects of mass transfer during droplet formation, rise, and coalescence (Kreager and Geankoplis, 1953). The solid lines were calculated from Eq. 6, values of α being determined by linear regression on Eq. 8, which yielded straight lines intercepting at the origin. The experimental results show a generally linear increase in droplet protein concentration with height over the distances investigated, and there appears to be reasonable agreement between Eq. 6 and the experimental data. Calculated values of the overall mass-transfer coefficient, K_L, using Eq. 6 are in the range 7.6×10^{-7} ms^{-1} ($t=1$ min) to 4.2×10^{-7} ms^{-1} ($t=30$ min).

The extraction of protein from the continuous phase at various dispersed-phase flow rates is shown in Figure 6. The solid lines represent values calculated from Eq. 10, which gives good agreement between all the experimental and calculated extraction profiles, the normalized standard deviation being $<10\%$. Over the duration of each experiment there is a generally linear decrease in protein concentration that is greater at higher dispersed phase flow rates due to the increased volume of the dispersed phase being passed through the column. For dispersed phase flow rates of 1.3, 3.3 and and 5.3 mL/min, the calculated values of K_L are 7.5, 5.6 and 3.91×10^{-7} ms^{-1}, respectively, that is, K_L decreases with increasing Q. These values of K_L represent average values over the duration of each experiment and are of the same order of magnitude as those calculated using concentration height data. The agreement between K_L values determined using both Eq. 6 and Eq. 10 would appear to confirm the validity of the model.

Theoretically, it would be expected that K_L is constant during the course of each experiment and would increase with increasing dispersed phase flow rate, Q. However, as indicated by the calculated values of K_L from the data presented in Figures 5 and 6, this is clearly not the case. The calculated decrease in K_L values with increasing Q and t is probably due to increasing backmixing of the continuous phase (Pratt and Stevens, 1992). Although the continuous phase is assumed to be stagnant in this work, the increasing drag in the wake of the rising (or falling) droplets will cause increased mixing of the continuous phase with increasing Q. This will then reduce the effective concentration driving force, and hence decrease the calculated value of K_L. The effects of such backmixing, or axial dispersion, on the concentration driving forces in such a column have been described by Pratt and Stevens (1992). These results would suggest that the assumption of a stagnant continuous phase is an over simplification in the development of the model.

Forward extraction of lysozyme during semibatch operation

The effects of aqueous phase ionic strength and dispersed-phase flow rate on the measured values of the overall mass-transfer coefficient, K_L, are shown in Table 3 both for dispersed reverse micelle phases and dispersed aqueous phases. Values of K_L were calculated from data relating to the change in continuous phase protein concentration with time according to Eq. 10. The decline in K_L values with increasing ionic strength is consistent with earlier findings (Lye et al., 1994a), which showed that at higher ionic strengths, electrostatic interactions between the protein molecules and the reverse micellar droplets are more effectively screened, and consequently that the rate of protein partitioning is reduced. High ionic strengths would also be expected to reduce the rate and extent of protein solubilization by causing a reduction in micelle size (as indicated by the decrease in W_0 values in Table 1). The tendency for K_L values to either decrease or remain essentially constant with

Table 3. Effect of Dispersed Phase Type and Flow Rate Either Ionic Strength (top) or pH (bottom) on the Overall Mass Transfer Coefficient, K_L*

DP Flow	Measured Overall MT Coefficients $K_L \times 10^7$ (ms^{-1})					
	0.2 M		0.3 M		0.4 M	
(mL/min)	Disp-RM	Disp-AQ	Disp-RM	Disp-AQ	Disp-RM	Disp-AQ
1.3	7.51	4.24	5.23	3.80	4.64	0.70
2.5	5.54	4.79	4.43	3.35	3.39	0.90
3.3	5.56	5.11	4.18	2.92	2.73	1.14
4.3	5.46	5.06	3.15	3.28	2.09	0.82
5.3	3.91	4.73	2.80	2.97	1.89	0.99
DP Flow	Measured Overall MT Coefficients $K_L \times 10^7$ (ms^{-1})					
	pH 7.0		pH 9.4		pH 10.6	
(mL/min)	Disp-RM	Disp-AQ	Disp-RM	Disp-AQ	Disp-RM	Disp-AQ
1.3	7.51	4.24	6.95	5.34	1.87	2.02
2.5	5.54	4.79	5.98	5.54	1.38	2.78
3.3	5.56	5.11	5.00	6.02	1.38	3.16
4.3	5.46	5.06	5.11	6.43	1.07	3.35
5.3	3.91	4.73	4.90	6.33	1.10	2.64

*Aqueous phase initially consisted of 0.5 mg/mL lysozyme in 90% KCl/10% buffer adjusted to the desired pH and ionic strength while the organic phase consisted of 50 mM AOT in isooctane. Column height was 30 cm.

increasing dispersed phase flow rate is probably due to backmixing of the continuous phase as described earlier. It is also clear from Table 3 that, under identical conditions, faster mass-transfer rates are found when the micellar phase is dispersed. Given that stagnant droplets are formed in both cases, this could be due to the more rapid diffusion of protein away from the interface in the case of the organic phase droplets (see the calculated values of D_{aq} and D_{rm} obtained later using Eq. 26).

The effects of aqueous-phase pH and dispersed-phase flow rate, either aqueous or organic, on the mass-transfer rate of lysozyme are also shown in Table 3. In earlier work on well-mixed systems (Lye et al., 1994a), the mass-transfer rate of lysozyme was found to decrease with increasing pH. This was attributed to a decrease in the magnitude of electrostatic interactions between protein and surfactant molecules, which occurred as the pH was increased. At low pH values, far removed from the protein's isoelectric point (pI), the surface of the lysozyme molecule will have a large overall positive charge and will therefore interact strongly with the negatively charged surfactant head-groups. Similar results are displayed for the spray column system in Table 3, except that K_L values for experiments at pH 7.0 and pH 9.4 are not widely different (the standard deviation associated with K_L determination is 0.3). This could perhaps be explained by reference to the titration curve of lysozyme (Tanford and Wagner, 1954), which shows that there is only a relatively small variation in protein charge over this pH range. The tendency for K_L to decrease with increasing dispersed-phase flow rate is again considered to be due to backmixing of the continuous phase, and K_L values are again seen to be generally larger in cases where the organic, rather than the aqueous, phase is dispersed.

Changes in the water content of the reverse micelle phases during column operation, when the micellar phase was either dispersed or continuous, are reported elsewhere (Lye, 1993). The values of W_0 were found to be virtually independent of dispersed-phase flow rate as would be expected for phases that had been preequilibrated and given the small changes in protein concentration occurring during extraction. The decline in W_0 with increasing ionic strength was again explained by the increased screening of electrostatic charges at higher ionic strengths, which leads to a reduction in micelle size.

Prediction of individual mass-transfer coefficients

Although numerous studies have been performed on mass transfer in liquid–liquid spray columns (Rostami Jafarabad et al., 1990), interfacial tensions have typically been in the range 8–50 mN m^{-1}. These are considerably higher than those found between aqueous and reverse micellar phases (Aveyard et al., 1986), which are of the order of 1–2 mN m^{-1} (Table 2). The presence of surface active agents can be predicted to reduce mass transfer in liquid–liquid systems by reducing the internal circulation and terminal velocities of the drops (as described earlier), and by acting as a barrier to transport across the interface. Thus, it is necessary to use mass-transfer correlations developed for surfactant-containing systems rather than to simply enter the reduced values of interfacial tension in surfactant-free correlations (Skelland, 1992). One potential problem with this, however, is that the available correlations have been developed almost exclusively for systems containing surfactants well below their critical micelle concentrations (cmc). For the reverse micelle phases used in this work, surfactant concentrations are necessarily greater than the cmc value; thus, the interface between the two bulk phases can be expected to be in a condensed rather than an expanded state. Thus, the resistance to mass transfer caused by the surfactant concentrations used here may well be greater than accounted for in the following correlations. Furthermore, to obtain theoretically consistent estimates of K_L, the mass-transfer processes occurring during drop formation, free rise (or fall), and coalescence must also be taken into account. Skelland (1992) has reviewed the appropriate correlations for obtaining "crude" estimates of the dispersed phase (k_{df}, k_{dr}, k_{dc}) and continuous phase (k_{cf}, k_{cr}, k_{cc}) mass-transfer coefficients in surfactant-containing systems.

For mass transfer during drop formation, assuming that droplet size increases by the addition of fresh elements,

Heertjes and coworkers developed the following correlation for the dispersed phase mass-transfer coefficient, k_{df} (Skelland, 1992):

$$k_{df} = 3.429\left(\frac{D_d}{\pi t_f}\right)^{1/2}, \tag{19}$$

which is based upon the solute diffusion coefficient in the dispersed phase, D_d, and the time of droplet formation, t_f (the value of t_f is calculated here by dividing the measured drop volume by the volumetric flow rate of the dispersed phase through each nozzle). The corresponding continuous-phase mass-transfer coefficient during drop formation, k_{cf}, is obtained by replacing D_d with D_c.

For mass transfer during droplet free rise (or fall), correlations for both dispersed- and continuous-phase mass-transfer coefficients, k_{dr} and k_{cr}, have been proposed for situations in which the fluid inside the dispersed-phase droplets is either stagnant or circulating (Skelland and Conger, 1973). Mass transfer will be faster for circulating drops since the solute is constantly transferred to, and removed from, the interface. For stagnant drops, the following correlations have been proposed by Vermeulen (1953) and Skelland and Cornish (1963), respectively:

$$k_{dr} = -\frac{d_e U_s}{6H_d}\ln\left[1 - \frac{2\pi D^{0.5} H_d^{0.5}}{d_e U_s^{0.5}}\right] \tag{20}$$

$$k_{cr} = 0.74\frac{D}{d_e}\left[\frac{d_e U_s \rho_c}{\mu_c}\right]^{0.5}\left[\frac{\mu_c}{\rho_c D}\right]^{0.33}. \tag{21}$$

For circulating drops, the following correlations have been proposed by Skelland and Wellek (1964) and Ruby and Elgin (1955), respectively, and Treybal (1963):

$$k_{dr} = 31.4\frac{D}{d_e}\left[\frac{4DH_d}{U_s d_e^2}\right]^{-0.34}\left[\frac{\mu_d}{\rho_d D}\right]^{-0.125}\left[\frac{d_e U_s^2 \rho_c}{\sigma}\right]^{0.37} \tag{22}$$

$$k_{cr} = 0.725\frac{D}{d_e}\left[\frac{d_e U_s \rho_c}{\mu_c}\right]^{0.57}\left[\frac{\mu_c}{\rho_c D}\right]^{0.42}(1-\epsilon_d) \tag{23}$$

where d_e is an equivalent drop diameter (based on the volume of an equivalent sphere), H_d is the height of the dispersion, D is the diffusion coefficient of the protein in the phase under consideration, and σ is the interfacial tension. The density and viscosity of the dispersed and continuous phases are ρ_d, μ_d, and ρ_c, μ_c respectively; and U_s is the slip velocity calculated from

$$U_s = U_t(1-\epsilon_d), \tag{24}$$

where U_s is the terminal velocity of the droplet and ϵ_d is the specific dispersed phase holdup. In our earlier work, when we considered only mass transfer during droplet free rise (or fall), it was found that the correlations developed for stagnant drops gave the closest predictions to the observed mass-transfer rates (Lye et al., 1994b). This would be consistent with the fact that the droplets had diameters, d_e, between 1 and 2 mm and that there is a considerable quantity of surfactant present in the system (Handlos and Baron, 1957; Garner and Skelland, 1955). Given that the study on droplet hydrodynamics just cited also suggested that both dispersed aqueous and organic phase droplets were stagnant, then only the preceding correlations for k_{dr} and k_{cr} in the case of stagnant drops will be considered here.

For mass transfer during drop coalescence, Johnson and Hamielec developed the following correlation for the dispersed-phase mass-transfer coefficient, k_{dc} (Skelland, 1992):

$$k_{dc} = 2\left(\frac{D_d}{\pi t_f}\right)^{1/2}, \tag{25}$$

which is based upon the solute diffusion coefficient in the dispersed phase, D_d, and the time of droplet formation, t_f (calculated as for Eq. 19). The corresponding continuous-phase mass-transfer coefficient during drop coalescence, k_{cc}, is again obtained by replacing D_d with D_c. This expression is based upon the arrival of each drop at the coalescence plane and the subsequent transfer as the drop spreads over this plane. It is particularly suited to systems such as those used in this work where the coalescence process is virtually instantaneous.

In all of the preceding equations, the solute diffusion coefficient is an important parameter. To account for the different viscosities of the two phases and the size of the protein-reverse micelle complex, the diffusion coefficient of the protein in each phase was estimated form the correlation of Tyn and Gussek (1990):

$$D = \frac{(5.78\times10^{-8})T}{\mu R_g}, \tag{26}$$

where T is the absolute temperature, R_g is the radius of gyration of the protein (taken as 15.2 Å for lysozyme in aqueous solution), and the numerical constant has units $cm^2 s^{-1}$ cP Å K^{-1}. Since the viscosity of the aqueous phase showed little variation with experimental conditions (see Table 1), an average value of the aqueous phase lysozyme diffusion coefficient, $D_{aq} = 1.1\times10^{-10}$ $m^2 s^{-1}$, was used in Eqs. 19–25. In the case of reverse micelle phases, however, the value of R_g used in Eq. 26 should be the radius of the protein-reverse micelle complex rather than that of the protein alone. This is because in reverse micelle phases the protein is known to reside solely within the water pools of the reverse micelles rather than in the bulk solvent. Knowing the water content of the reverse micelle phase (i.e., the value of W_0 given in Table 2) and the size of the AOT molecule, then it is possible to calculate the radius of the protein-reverse micelle complex and hence the values of D_{rm} shown in Table 4 for use in Eqs. 19–25 (Lye, 1993; Mat, 1994). While the lower viscosity of the organic phase would be expected to increase the diffusivity of the protein, by taking into account the size of the protein-reverse micelle complex, it is seen in Table 3 that values of D_{rm} are only slightly larger than D_{aq}. This is in contrast to our earlier work (Lye et al., 1994b), where, by only considering the size of the protein in the reverse micellar phase rather

Table 4. Calculated Lysozyme Diffusion Coefficients in the Reverse Micelle Phases*

RM Phase Lysozyme Diffusion Coefficient, D_{rm} ($\times 10^{10}$) $m^2 s^{-1}$			
Ionic Strength (M)	Calc. D_{rm}	pH	Calc. D_{rm}
0.2	1.34	7.0	1.34
0.3	1.47	9.4	1.28
0.4	1.56	10.6	1.24

*D_{rm} values were calculated from Eq. 26 using the appropriate W_0 values from Table 1 to first calculate the size of the protein-reverse micelle complex.

than the protein-reverse micelle complex, the calculated value of D_{rm} was approximately twice D_{aq}.

Formulation of an overall mass-transfer coefficient

The formulation of an overall mass-transfer coefficient, K_L, from the individual dispersed (k_{df}, k_{dr}, k_{dc}) and continuous (k_{cf}, k_{cr}, k_{cc}) phase mass-transfer coefficients has recently been presented by Skelland (1992). This is based upon the individual mass-transfer coefficients and the interfacial area available for mass-transfer during each process. The expressions for the overall dispersed phase, k_{do}, and continuous phase, k_{co}, mass-transfer coefficients are

$$k_{do}aV_c = k_{df}A_f + k_{dr}A_r + k_{dc}A_c \tag{27}$$

$$k_{co}aV'_c = k_{cf}A'_f + k_{cr}A'_r + k_{cc}A'_c, \tag{28}$$

where A_f, A_r, and A_c are the respective interfacial areas available for mass transfer during drop formation, free rise (or fall), and coalescence with respect to the dispersed phase, while the primed symbols refer to the corresponding areas for the continuous phase. In the column used here, the interfacial areas available for mass transfer for the dispersed and continuous phases are equal and are calculated from the following expressions:

$$A_f = n_o \pi d_e^2 \tag{29}$$

$$A_r = \frac{H_c}{U_t t_f} n_o \pi d_e^2 \tag{30}$$

$$A_c = \frac{\pi d_{col}^2}{4}, \tag{31}$$

where n_o is the number of nozzles in the distributor, H_c is the height of free rise (or fall) of a droplet at terminal velocity, U_t, and d_{col} is the diameter of the column. The advantage of the approach described by Eqs. 27–31 is that it will permit estimates of the proportion of mass transfer occurring during the respective processes of droplet formation, free rise (or fall), and coalescence. Once the overall dispersed and continuous-phase mass-transfer coefficients have been determined, they can be used to formulate an overall mass-transfer coefficient as defined in Eq. 4. For experiments in which the reverse micelle phase is dispersed, the overall mass-transfer coefficient, K_L, can be calculated from

$$\frac{1}{K_L} = \frac{1}{k_{rm}} + \frac{1}{mk_{aq}} = \frac{1}{k_{do}} + \frac{1}{mk_{co}} \tag{32}$$

if it is again assumed that mass transfer is limited by diffusion in one or other of the boundary-layer films rather than by an interfacial solubilization process.

Comparison of predicted and measured overall mass-transfer coefficients

For each of the experiments performed in Table 3, values of the individual mass-transfer coefficients, k_{df}, k_{dr}, k_{dc}, k_{cf}, k_{cr}, and k_{cc} were predicted from the appropriate physical property data, column dimensions, and the measured droplet sizes and terminal velocities using Eqs. 19–21 and 24–26. A predicted value of the overall mass-transfer coefficient, K_L, was then obtained by the procedure outlined in Eqs. 27–32 using an appropriate value of the experimentally determined equilibrium partition coefficient, m, from Table 2. The predicted values of K_L are given in Table 5. Note that if a suitable thermodynamic theory were available for predicting the value of m, then by using values of V_d (from Eq. 13) and U_t (from Eqs. 14–15), it would be possible to predict K_L values knowing only the physical properties of the phases and the conditions under which the spray column was to be operated.

The most striking feature of the predicted values of K_L given in Table 5 is that they are generally between 2 and 10 times greater than the experimentally determined values (cf. Table 3). As was suggested earlier, this is probably due to the large concentration of surfactant used in the reverse micellar systems. It would appear that use of AOT concentrations above the cmc leads to the formation of a larger interfacial barrier (and hence more internally stagnant droplets) than was present in the systems from which the employed correlations were developed. If diffusive transport in the stagnant droplets is an important phenomenon, as is suggested by the results presented so far, another possible source of error relates to the nature of the solute being transferred. The molecular mass of lysozyme is 3 to 4 orders or magnitude greater than the solutes used to develop the preceding correlations, and hence the values of D_{aq} or D_{rm} will be considerably different, for example, for the water-acetic acid-toluene system, the diffusion coefficient of the solute is approximately 2.3×10^{-9} $m^2 \cdot s^{-1}$. For this system, it was also found that surfactants could reduce k_d values to 10% of the value found in surfactant-free experiments (Skelland and Caenepeel, 1972). For the systems used here, then, the combination of a packed surfactant interface and the small diffusion coefficient of the solute being transferred, are thought to be the main reasons for the overprediction of K_L values.

Another erroneous feature of the predicted K_L values shown in Table 5, is that they increase with increasing aqueous phase pH and ionic strength. This is entirely opposite to the trends found experimentally. Since the column was operated over a limited range of flow rates and with phases having reasonably similar physical properties, the trend observed in the predicted K_L values with increasing ionic strength is probably a result of the calculated D_{rm} values given in Table 4. Due to the smaller micelles formed at high ionic strength (see W_0 values in Table 1), the calculated values of D_{rm} are seen to increase. While this is acceptable physically, what the

Table 5. Predicted Values of the Overall Mass-Transfer Coefficient, K_L, Corresponding to Phase Properties and Column Operating Conditions in Table 3*

DP	Predicted Overall MT Coefficients $K_L \times 10^7$ (ms^{-1})					
Flow	0.2 M		0.3 M		0.4 M	
(mL/min)	Disp-RM	Disp-AQ	Disp-RM	Disp-AQ	Disp-RM	Disp-AQ
1.3	14.0	13.2	11.8	13.0	22.5	30.1
2.5	12.2	10.5	10.3	10.2	20.0	27.1
3.3	10.7	9.50	11.2	8.00	19.0	22.7
4.3	10.3	8.40	9.30	7.20	21.6	18.5
5.3	13.1	7.50	9.90	8.00	19.5	16.3
DP	Predicted Overall MT Coefficients $K_L \times 10^7$ (ms^{-1})					
Flow	pH 7.0		pH 9.4		pH 10.6	
(mL/min)	Disp-RM	Disp-AQ	Disp-RM	Disp-AQ	Disp-RM	Disp-AQ
1.3	14.0	13.2	16.5	15.8	23.2	22.7
2.5	12.2	10.5	13.8	13.2	21.2	19.5
3.3	10.7	9.50	12.7	10.5	18.8	18.7
4.3	10.3	8.40	13.3	9.6	21.0	13.7
5.3	13.1	7.50	11.9	9.00	17.1	15.1

*Values of K_L were calculated as described in Eqs. 19–23 and 27–32.

correlations cannot describe is the associated decrease in the magnitude of the electrostatic protein–micelle interactions that occur at high pH and ionic strength. Unfortunately, these electrostatic interactions cannot be represented by the value of m in Eq. 32, since it has been shown that the extraction kinetics are independent of m over the pH range investigated (Lye et al., 1994a). It is also at these high values of pH and ionic strength that the largest discrepancy exists between the predicted and measured values of K_L. Another possible reason for this is that under conditions of high pH and ionic strength, the kinetics of the interfacial solubilization process may become sufficiently slow that this is the rate-limiting step (Dungan et al., 1991). It would therefore become necessary to include an interfacial solubilization term in Eq. 32.

Given the predicted values of K_L in Table 5, a comparison of the experimental and predicted extraction profiles for the change in continuous-phase protein concentration with time is shown in Figure 7 for the case of a dispersed aqueous phase. The particular case illustrated corresponds to the average error between experimental and predicted K_L values. As expected, the predicted increase in continuous-phase protein concentration is approximately three times faster than is found experimentally. While it thus appears to be impossible to predict K_L values in reverse micellar systems using existing correlations, certain trends were qualitatively predicted, namely that K_L will be greater in the case of dispersed reverse micelle phases and at lower dispersed-phase flow rates. If further attempts are made to predictively model reverse micellar mass-transfer processes, it would therefore seem clear that it will also be necessary to account for the variation of electrostatic protein–micelle interactions with phase composition.

Analysis of protein transfer during drop formation, rise (or fall), and coalescence

Although it was only possible to predict overall K_L values to within an order of magnitude, the approach outlined in Eqs. 27–32 did provide some useful insights into the likely proportions of solute being extracted during the successive processes of droplet formation, free rise (or fall), and coalescence. Representative values of the individual mass-transfer coefficients and areas available for mass transfer are given in Table 6 for the case of a dispersed reverse micelle phase at three different flow rates. The figures in parentheses represent the percentage of protein being transferred during each stage. An identical picture of events was found for the case of dispersed aqueous phases.

From the relative values for k_f, k_r, and k_c, it appears that a significant proportion of solute should be extracted during the droplet-formation and coalescence processes as opposed to the free rise stage. This is particularly true considering the small height of the spray column employed. However, when the magnitudes of A_f, A_r, and A_c are considered, it is clear that the large values of both k_c and A_c will mean that the most significant proportion of protein will be extracted during the droplet coalescence process. The figures given in Table 6 suggest that this may be up to 70–80% of the total protein extracted at low dispersed-phase flow rates. How-

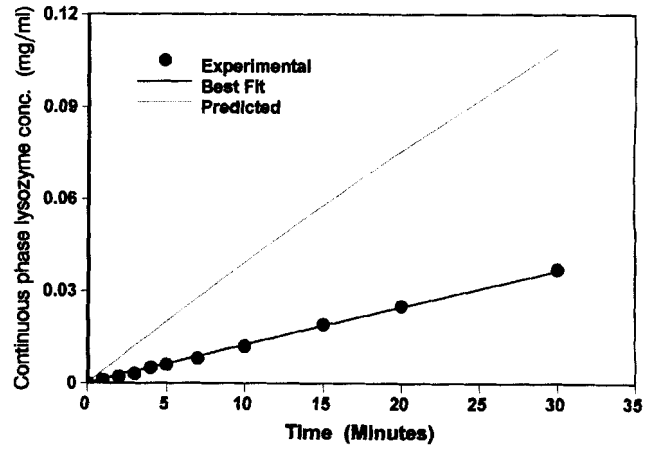

Figure 7. Experimental vs. predicted extraction profiles for the dispersed aqueous phase.

Phase compositions as in Figure 6, column height was 30 cm and the dispersed phase flow rate was 1.3 mL/min.

Table 6. Predicted Mass-Transfer Coefficients with Dispersed-Phase Flow Rate for (top) Dispersed Phase and (bottom) Continuous Phase*

DP Flow (mL/min)	$k_{df} \times 10^5$ (ms^{-1})	$k_{dr} \times 10^5$ (ms^{-1})	$k_{dc} \times 10^5$ (ms^{-1})	$A_f \times 10^4$ (m^2)	$A_r \times 10^4$ (m^2)	$A_c \times 10^4$ (m^2)	a (m^2/m^3)	$k_{do} \times 10^5$ (ms^{-1})
1.3	5.4	0.67	3.15	0.18 (5.2)	4.03 (14.0)	4.91 (80.8)	2.5	5.21
3.3	7.46	0.65	4.35	0.22 (5.7)	9.51 (21.3)	4.91 (73.0)	5.3	3.75
5.3	9.95	0.64	5.8	0.21 (5.0)	16.9 (26.0)	4.91 (69.0)	6.4	4.39
DP Flow (mL/min)	$k_{cf} \times 10^5$ (ms^{-1})	$k_{cr} \times 10^5$ (ms^{-1})	$k_{cc} \times 10^5$ (ms^{-1})	$A'_f \times 10^4$ (m^2)	$A'_r \times 10^4$ (m^2)	$A'_c \times 10^4$ (m^2)	a (m^2/m^3)	$k_{co} \times 10^5$ (ms^{-1})
1.3	4.9	1.35	2.86	0.18 (4.4)	4.03 (26.7)	4.91 (68.9)	2.5	5.55
3.3	6.76	1.27	3.94	0.22 (4.6)	9.51 (36.7)	4.91 (58.7)	5.3	4.23
5.3	9.01	1.25	5.24	0.21 (3.9)	16.9 (43.3)	4.91 (52.8)	6.4	5.19

*The proportions of mass transfer occurring during drop formation, free rise, and coalescence are given as percentages in parentheses. Values calculated using Eqs. 19–32 in the case of a dispersed reverse micelle phase at pH 7 and an ionic strength of 0.2 M.

ever, given the error in the prediction of the overall K_L values, these figures should only be used to convey trends and not absolute quantities. With increasing dispersed-phase flow rate, Q, it is also seen in Table 6 that the estimated values of k_f and k_c increase, while k_r changes very little. This is due to the associated decrease in the droplet formation time, t_f, which is an important parameter in calculating k_f and k_c using Eqs. 19 and 26, respectively. However, due to the increased holdup of the dispersed phase, there is a large increase in A_r such that at high Q, a substantial fraction of the protein is extracted during the free rise stage. These figures will be important when considering the design and modeling of spray columns using reverse micellar phases.

Summary and Conclusions

It has been demonstrated that protein extraction using reverse micellar phases can be successfully carried out in a liquid–liquid spray column. When operated in a semibatch mode, the presence of surfactant in the organic phase did not lead to problems of emulsion formation within the column. This type of contactor therefore provides one route by which reverse micellar extraction processes may be scaled up.

The spray-column model developed here satisfactorily described the kinetics of protein extraction. Good agreement was found between experimental and calculated extraction profiles for both the change in droplet protein concentration with height and also for the change in continuous-phase protein concentration with time. This further suggests that the two-film theory of mass transfer can be applied to protein extraction using reverse micellar systems. Assumptions concerning the mixedness of the continuous phase appear to be the major uncertainty in the development of the model. Values of K_L determined over a range of experimental conditions showed that the rate of lysozyme mass transfer decreased with increasing pH and increasing ionic strength as has been found in other systems (Dekker et al., 1990; Lye et al., 1994a). Measured K_L values generally showed little variation over the range of dispersed-phase flow rates in which discrete droplets could be formed, while the properties of the dispersed phase were found to have a significant effect on the rate of protein mass transfer.

Study of the droplet hydrodynamics suggested that the presence of AOT increased the rigidity of the two-phase interface resulting in the formation of stagnant droplets. This fact was important when selecting appropriate correlations for predicting mass-transfer coefficients for the droplet formation, free rise (or fall), and coalescence processes. The presence of high interfacial surfactant concentrations is also thought to be the reason why the predicted K_L values were consistently higher than the measured ones. Calculation of the individual mass-transfer coefficients and interfacial areas during the individual formation, free rise (or fall), and coalescence processes provided useful information concerning the proportions of solute transferred in each step.

Acknowledgments

The authors would like to thank the SERC in conjunction with the AFRC Institute of Food Research (Reading Laboratory) for financial support of this work (CASE award for G.J.L.). Useful comments from one of the reviewers regarding the formulation of the overall mass-transfer coefficient were also appreciated.

Notation

a = specific interfacial area ($m^2 \cdot m^{-3}$)
d = equatorial droplet diameter (m)
g = gravitational acceleration (ms^{-2})
k_{rm}, k_{aq} = overall individual film mass-transfer coefficient (ms^{-1})

Subscripts and superscripts

d = dispersed phase/disperser/droplet
i = interface

Literature Cited

Aveyard, R., B. P. Binks, S. Clark, and J. Mead, "Interfacial Tension Minima in Oil-Water-Surfactant Systems," *J. Chem. Soc., Farad. Trans. I*, **82**, 125 (1986).

Bhawsar, P. C. M., A. B. Pandit, S. B. Sawant, and J. B. Joshi, "Enzyme Mass Transfer Coefficient in a Sieve Plate Extraction Column," *Chem. Eng. J.*, **55**, B1 (1994).

Binks, B. P., J. Meunier, O. Abillon, and D. Langevin, "Measure-

ment of Film Rigidity and Interfacial Tensions in Several Ionic Surfactant-Oil-Water Microemulsion Systems," *Langmuir*, **5**, 415 (1989).
Carneiro-da-Cunha, M. G., M. R. Aires-Barros, E. B. Tambourgi, and J. M. S. Cabral, "Recovery of a Recombinant Cutinase with Reverse Micelles in a Continuous Perforated Rotating Disc Contactor," *Biotech. Tech.*, **8**, 413 (1994).
Clift, R., J. R. Grace, and M. E. Weber, *Bubbles, Drops and Particles*, Academic Press, New York (1978).
Dahuron, L., and E. L. Cussler, "Protein Extractions with Hollow Fibers," *AIChE J.*, **34**, 130 (1988).
Dekker, M., P. H. M. Koenen, and K. Van't Riet, "Reversed Micellar-Membrane-Extraction of Enzymes," *Trans. Ind. Chem. Eng.*, **69(C)**, 54 (1991a).
Dekker, M., K. Van't Riet, B. H. Bijsterbosch, P. Fijneman, and R. Hilhorst, "Mass Transfer Rate of Protein Extraction with Reversed Micelles," *Chem. Eng. Sci.*, **45**, 2949 (1990).
Dekker, M., K. Van't Riet, J. J. Van Der Pol, J. W. A. Baltussen, R. Hilhorst, and B. H. Bijsterbosch, "Effect of Temperature on the Reversed Micellar Extraction of Enzymes," *Chem. Eng. J.*, **46**, B69 (1991b).
Dekker, M., K. Van't Riet, S. R. Weijers, J. W. A. Baltussen, C. Laane, and B. H. Bijsterbosch, "Enzyme Recovery by Liquid-Liquid Extraction Using Reverse Micelles," *Chem. Eng. J.*, **33**, B27 (1986).
Dungan, S. R., T. Bausch, T. A. Hatton, P. Plucinski, and W. Nitsch, "Interfacial Transport Processes in the Reversed Micellar Extraction of Protein," *J. Colloid Interf. Sci.*, **145**, 33 (1991).
Garner, F. H., and A. H. P. Skelland, "Some Factors Affecting Droplet Behaviour in Liquid-Liquid Systems," *Chem. Eng. Sci.*, **4**, 149 (1955).
Grace, J. R., T. Wairegi, and T. H. Nguyen, "Shapes and Velocities of Single Drops and Bubbles Moving Freely Through Immiscible Liquids," *Trans. Inst. Chem. Eng.*, **54**, 167 (1976).
Han, D. H., S. Y. Lee, and W. H. Hong, "Separation of Intracellular Proteins from *Candida Utilis* Using Reverse Micelles in a Spray Column," *Biotech. Tech.*, **8**, 105 (1994).
Handlos, A. E., and T. Baron, "Mass and Heat Transfer from Drops in Liquid-Liquid Extraction," *AIChE J.*, **3**, 127 (1957).
Hayworth, C. B., and R. E. Treybal, "Drop Formation in Two-Liquid-Phase Systems," *Ind. Eng. Chem.*, **42**, 1174 (1950).
Hu, S., and R. C. Kintner, "The Fall of Single Liquid Drops through Water," *AIChE J.*, **1**, 42 (1955).
Kinugasa, T., S. I. Tanahashi, and H. Takeuchi, "Extraction of Lysozyme Using Reversed Micellar Solution: Distribution Equilibria and Extraction Rates," *Ind. Eng. Chem. Res.*, **30**, 2470 (1991).
Klee, A. J., and R. E. Treybal, "Rate of Rise or Fall of Liquid Drops," *AIChE J.*, **2**, 444 (1956).
Kreager, R. M., and C. J. Geankoplis, "Effect of Tower Height in a Solvent Extraction Tower," *Ind. Eng. Chem.* **45**, 2156 (1953).
Lo, T. C., "Commercial Liquid-Liquid Extraction Equipment," *Handbook of Separation Techniques for Chemical Engineers*, P. A. Schweitzer, ed., McGraw-Hill, New York (1988).
Luthi, P., and T. A. Hatton, "Recovery of Biocatalysis Products from Reversed Micellar Reaction Media: A Preliminary Evaluation of Membrane Extractors," *Bioseparation*, **2**, 5 (1991).
Lye, G. J., "Kinetic Studies on the Extraction and Separation of Proteins Using Reverse Micelles," PhD Thesis, Univ. of Reading, Reading, U.K. (1993).
Lye, G. J., J. A. Asenjo, and D. L. Pyle, "Protein Extraction Using Reverse Micelles: Kinetics of Protein Partitioning," *Chem. Eng. Sci.*, **49**, 3195 (1994a).
Lye, G. J., J. A. Asenjo, and D. L. Pyle, "Kinetics of Protein Extraction Using Reverse Micelles: Studies in Well-Mixed Systems and a Liquid-Liquid Spray Column," *Separations for Biotechnology 3*, D. L. Pyle, ed., SCI Publishing, London (1994b).
Mat, H. B., "Protein Extraction Using Reverse Micelles: System Parameters and Mass Transfer Studies," PhD Thesis, Univ. of London, London, U.K. (1994).
Plucinski, P., and W. Nitsch, "Two-Phase Kinetics of the Solubilization in Reverse Micelles—Extraction of Lysozyme," *Ber. Bunsenges. Phys. Chem.*, **93**, 994 (1989).
Pratt, H. R. C., and G. W. Stevens, "Axial Dispersion," *Science and Practice of Liquid-Liquid Extraction*, J. D. Thornton, ed., Clarendon Press, Oxford (1992).
Prazeres, D. M. F., F. A. P. Garcia, and J. M. S. Cabral, "An Ultrafiltration Membrane Bioreactor for the Lipolysis of Olive Oil in Reversed Micellar Media," *Biotechnol. Bioeng.*, **41**, 761 (1993).
Rostami Jafarabad, K., J. B. Joshi, and D. D. Kale, "Effect of Viscosity and Drag Reducing Agents on Mass Transfer in Liquid-Liquid Spray Columns," *Solv. Ext. Ion Exch.*, **8**, 669 (1990).
Rostami Jafarabad, K., S. B. Sawant, J. B. Joshi, and S. K. Sikdar, "Enzyme and Protein Mass Transfer Coefficient in Aqueous Two-Phase Systems. I. Spray Extraction Columns," *Chem. Eng. Sci.*, **47**, 57 (1992).
Ruby, C. L., and J. C. Elgin, "Mass Transfer between Liquid Drops and a Continuous Liquid Phase in a Countercurrent Fluidized System: Liquid-Liquid Extraction in a Spray Tower," *Chem. Eng. Progr. Symp. Ser.*, No. 16, 17 (1955).
Scheele, G. F., and B. J. Meister, "Drop Formation at Low Velocities in Liquid-Liquid Systems: 1. Prediction of Drop Volume," *AIChE J.*, **14**, 9 (1968).
Skelland, A. H. P., "Interphase Mass Transfer," in *Science and Practice of Liquid-Liquid Extraction*," J. D. Thornton, ed., Clarendon Press, Oxford (1992).
Skelland, A. H. P., and C. L. Caenepeel, "Effects of Surface Active Agents on Mass Transfer during Droplet Formation, Fall, and Coalescence," *AIChE J.*, **18**, 1154 (1972).
Skelland, A. H. P., and W. L. Conger, "A Rate Approach to Design of Perforated-Plate Extraction Columns," *Ind. Eng. Chem. Process Des. Develop.*, **12**, 448 (1973).
Skelland, A. H. P., and A. R. H. Cornish, "Mass Transfer from Spheroids to an Air Stream," *AIChE J.*, **9**, 73 (1963).
Skelland, A. H. P., and R. M. Wellek, "Resistance to Mass Transfer Inside Droplets," *AIChE J.*, **10**, 491 and 789 (1964).
Skelland, A. H. P., S. Woo, and G. G. Ramsay, "Effects of Surface-Active Agents on Drop Size, Terminal Velocity, and Droplet Oscillation in Liquid-Liquid Systems," *Ind. Eng. Chem. Res.*, **26**, 907 (1987).
Tanford, C., and M. L. Wagner, "Hydrogen Ion Equilibria of Lysozyme," *J. Amer. Chem. Soc.*, **76**, 3331 (1954).
Treybal, R. E., *Liquid Extraction*, 2nd ed., McGraw-Hill, New York (1963).
Tyn, M. T., and T. W. Gusek, "Prediction of Diffusion Coefficients of Protein," *Biotechnol. Bioeng.*, **35**, 327 (1990).
Underwood, J. L., K. A. Debelak, and D. J. Wilson, "Soil Cleanup by *in-situ* Surfactant Flushing. VII. Determination of Mass Transfer Coefficients for Reclamation of Surfactant for Recycle," *Sep. Sci. Technol.*, **30**, 73 (1995).
Uribe, I. O., S. Wongswan, and E. S. Perez de Ortiz, "A Systematic Model for the Study of the Rate-Controlling Mechanisms in Liquid Membrane Permeation Processes. Extraction of Zinc by bis(2-Ethylhexyl)phosphoric Acid," *Ind. Eng. Chem. Res.*, **27**, 1696 (1988).
Vermeulen, T., "Theory for Irreversible and Constant-Pattern Solid Diffusion," *Ind. Eng. Chem.*, **45**, 1664 (1953).
Weast, R. C., *Handbook of Mathematical Tables*, 2nd ed., Chemical Rubber Co., Cleveland, OH (1964).
Weatherley, L. R., and C. Turmel, "Terminal Velocity Studies of Whole Broth Single Drops in a Liquid-Liquid System," *Ind. Eng. Chem. Res.*, **31**, 1739 (1992).

Manuscript received May 16, 1994, and revision received May 3, 1995.